Tunable Assembly of Block Copolymer Tethered Particle Brushes by SI-ATRP

Zongyu Wang^{†, §}, Jaejun Lee^{‡, §}, Zhenhua Wang^{†, ⊥,∇}, Yuqi Zhao[‡], Jiajun Yan^{†, ||}, Yu Lin[‡], Sipei Li[†], Tong Liu[†], Mateusz Olszewski[†], Joanna Pietrasik[∏], Michael R. Bockstaller^{*, ‡}, Krzysztof Matyjaszewski^{*, †}

§ Z.W. and J.L. contributed equally.

KEYWORDS: bimodal, particle brush, SI-ATRP, string-like structure

ABSTRACT: A strategy to synthesize SiO₂-*g*-PMMA/PMMA-*b*-PS mono- and bimodal block copolymer particle brushes by surface-initiated atom transfer radical polymerization (SI-ATRP) from silica particles is presented. First, PMMA blocks were prepared by normal ATRP with controlled degree of polymerizations and grafting density. In a second step, the PS block was synthesized through a chain extension using low-ppm Cu catalyst. Variation of the SiO₂-*g*-PMMA-Br macroinitiator concentration had a pronounced effect on the modality of the chain extension product. In the limit of small concentration, partial termination resulted in bimodal brush architectures while more uniform brush architectures were observed with increasing concentration of macroinitiator. Brush nanoparticles with bimodal architectures assembled into string-like aggregates that bear resemblance to structures found in systems comprised of sparse (homopolymer) brush particles. The unexpected effect of modality on structure formation points to opportunities in controlling microstructures in brush particle materials.

The grafting of polymer chains to the surface of nanoparticles to form so-called brush (or 'hairy') particles has emerged as a viable route to tailor the interactions, assembly behavior and properties of particulate materials. For example, the increased structural uniformity of particle brush-based hybrids in conjunction with the more stretched conformations in densely tethered brush systems was shown to raise the

dielectric breakdown strength and thermal transport or to result in novel phonon transport behavior.⁶ Properties of particle brush hybrids sensitively depend on the microstructure of the assembly.⁷⁻¹¹ Structural order and its dependence on the molecular characteristics of polymer canopies have thus been an important subject of recent research in this field.¹²⁻¹³ Two important parameters determining the structure of brush particle

[†]Department of Chemistry, Carnegie Mellon University, 4400 Fifth Avenue, Pittsburgh, Pennsylvania 15213

[‡]Department of Materials Science & Engineering, Carnegie Mellon University, 5000 Forbes Avenue, Pittsburgh, Pennsylvania 15213

 $^{^{\}perp}$ Xi'an Institute of Biomedical Materials and Engineering, Northwestern Polytechnical University, Xi'an, 710072, China

[▽] Institute of Flexible Electronics, Northwestern Polytechnical University, Xi'an, 710072, China

Ill Institute of Polymer and Dye Technology, Technical University of Lodz, Stefanowskiego 12/16, 90 924 Lodz, Poland

assemblies are the density and degree of polymerization (DP) of grafted chains. ¹⁴ In the dense grafting limit, hard sphere-type close packed assembly structures have been reported, mostly face-centered cubic (fcc). Long-range order was found to decrease with increasing degree of polymerization. In the sparse grafting limit (typically associated with grafting densities of the order of 0.01 chains/nm²) the formation of string-like superstructures was reported. ¹⁵⁻¹⁸ Interestingly, particle brush materials formed by string-like superstructures exhibited higher elastic moduli thus illustrating the opportunities for functional material design that are afforded by tailoring the structure of brush particle assemblies. ¹⁹

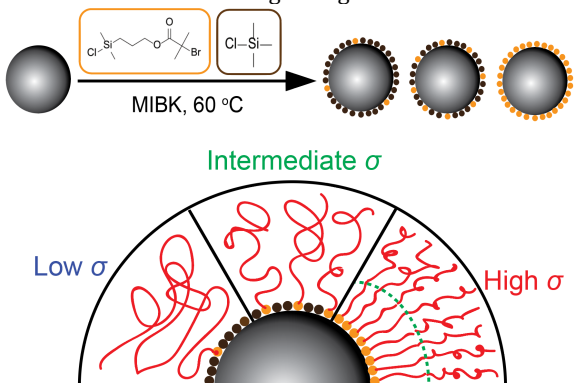
An interesting concept to widen the range of accessible microstructures in brush particle materials is by utilizing block copolymer (BCP) based ligands.²⁰⁻²¹ Since BCPs self-organize into a variety of microdomain structures (depending on composition and degree of polymerization), the structure in BCP-tethered brush materials is determined by the balance of hard spheretype interactions (contributed by the particle core) and the driving forces of BCP microdomain formation.²² The competition of the various driving forces for structure formation can be expected to give rise to a range of microstructures not typically found in homopolymer brush materials.²³⁻²⁴ Early indications of this 'phase space' were provided by numerical simulations of the assembly of particles tethered with single BCP chains.²⁵-²⁹ These simulations suggested that the presence of BCP tethers can result in the symmetry breaking of interactions and the formation of non-cubic assembly structures.³⁰⁻³⁶ To unravel the governing parameters that control structure formation in BCP-brush particle assemblies, synthesis has to accomplish control of a wide range of geometric and compositional parameters.³⁷⁻³⁸ In this letter, we present a strategy to synthesize SiO₂-g-PMMA/PMMA-b-PS bimodal block copolymer particle brushes by surface-initiated atom transfer radical polymerization (SI-ATRP) from silica particles. Here, 'bimodal' refers to the chain architecture obtained after partial extension of the primary PMMA graft layer. The bimodal architecture allows to selectively vary the density of copolymer chains while maintaining full coverage of particle cores by the primary polymer layer. This was seen as advantageous for correlating graft architectures with microstructure formation.

One key advantage of atom transfer radical polymerization (ATRP) is the possibility to prepare complex molecular architectures such as BCPs.³⁹⁻⁴⁰ The ability to control both the length scale and the spatial organization of BCP brush morphologies on nanoparticles makes these materials particularly attractive as scaffolds for the engineering of nanostructures.⁴¹⁻⁴³ For BCP-brush particles, we recently reported that deliberate choice of grafting density,

initiation efficiency, and initiator concentration enables tailoring of brush architecture from monomodal to bimodal (the term 'bimodal' generally refers to graft layers comprised of two populations of polymer chains of distinct molecular weights).44-45 This interdependence of grafting density, initiation efficiency and initiator concentration can be used to prepare BCP-tethered particle brushes with controlled degree of chain extension through simple chain extension reactions. In the following we demonstrate the possibility of controlling the degree of modality of the second block in copolymer-tethered particle brush systems and the respective effect on particle organization in thin films. Interesting differences between the assembly behavior of monomodal vs. bimodal BCP-brush particles are observed. While assembly structures of unimodal BCP particles resemble those of regular (homopolymer) brush particle systems, bimodal systems are found to assemble into string-like structures that bear resemblance to those predicted by simulation studies for mono-BCP-tethered particles. The intricate microstructure of these assembly structures could render these materials attractive as scaffolds for the engineering of nanostructures.46-48

The synthesis of monomodal SiO₂-g-PMMA-b-PS particle brushes was accomplished using surface-initiated atom transfer radical polymerization (SI-ATRP). First, PMMA blocks were "grafted from" the surface of the SiO₂ particles by normal SI-ATRP. Three SiO₂-Br nanoparticles were prepared for initial grafting of PMMA chains with controlled grafting densities (Table 1, Scheme 1). The grafting density was tuned by altering the ratio between tetherable ATRP initiator ((chlorodimethylsilyl)propyl α -bromoisobutyrate) and "dummy" initiator (chlorotrimethylsilane). The second PS block was formed using a low-ppm Cu catalyst ATRP procedure comprising of catalyst complexes with highly activating ligands.

Scheme 1. Synthesis of SiO₂-*g*-PMMA particle brushes with different grafting densities.



For the synthesis of bimodal copolymer particle brush with low grafting density, we utilized our previously reported finding that the bimodality of the particle brushes and the population of conjugated PS blocks can be tuned by altering the concentration of the particle pre-synthesized SiO₂-g-PMMA macroinitiators in the reaction.⁴⁴ Both low and high grafting density SiO₂-g-PMMA particle brush systems were used as substrates for the synthesis of bimodal BCP brush particles. However, stronger emphasis was given to lower grafting density systems. This is because it was expected that the reduced grafting density enables more efficient interactions between BCP tethers and hence microphase separation. Table 1 shows the composition of two sparsely grafted SiO2-g-PMMA particle brush systems that were synthesized by normal ATRP, PMMA-L1 with DP = 1335, grafting density 0.046 chains/nm² and PMMA-L2 with DP = 232, grafting density 0.042

chains/nm2, respectively. In order to achieve bimodal structures, low initiator concentrations of 20 and 40 ppm were used, for chain extension experiments with styrene monomers, samples M-b-S-1/2 (extended from PMMA-L1). After polymerization and purification, the samples were characterized by TEM and SEC. SEC traces of polymers cleaved from nanoparticles indicated clear bimodal features (Figures S6 and S7). The numberaveraged molecular weight (M_n) , dispersity and PMMA/PMMA-b-PS chain fractions were calculated by deconvolution of SEC traces. As shown in Table S3, under high target DP conditions, 50,000 and 25,000, only 7% and 11% of PMMA-Br chains were chain extended. Constant grafting density values before and after chain extensions suggested that the amount of free homopolymers generated from thermal-self initiation of styrene monomers was negligible.

Table 1. Result of syntheses of SiO₂-*g*-PMMA and SiO₂-*g*-PMMA-*b*-PS particle brushes with different grafting density and compositions

| and compositions | | | | | | | | |
|--------------------|----------------------|-------------------------|---------------------------|-----------|-----------------------------------|---------------|---|---|
| Entry ^a | M_{n}^{b} | $M_{\rm w}/M_{\rm n}^b$ | f_{ino} (%) c | σ (nm-2)d | <i>f</i> _{РММА} е (%) | σ1 (nm-2)f | <i>f</i> _{РММА-<i>b</i>-PS^{<i>e</i>} (%)} | σ ₂ (nm ⁻²) ^f |
| PMMA-H1 | 44,500 | 1.16 | 8.9 | 0.763 | | | | |
| PMMA-M1 | 56,300 | 1.12 | 26.2 | 0.165 | N/A | | | |
| PMMA-L1 | 133,500 | 1.18 | 35.1 | 0.046 | | | | |
| PMMA-L2 | 23,200 | 1.23 | 77.2 | 0.042 | | | | |
| PMMA-L3 | 47,700 | 1.13 | 57.7 | 0.051 | | | | |
| M- <i>b</i> -S-1 | 209,400 | 2.66 | 24.52 | 0.049 | 93.1 | 0.043 | 6.9 | 0.003 |
| M- <i>b</i> -S-2 | 241,800 | 2.11 | 24.15 | 0.044 | 88.6 | 0.039 | 11.4 | 0.005 |
| M- <i>b</i> -S-3 | 206,800 | 3.17 | 27.52 | 0.042 | 45.2 | 0.019 | 54.8 | 0.023 |
| M- <i>b</i> -S-4 | 80,600 | 1.68 | 21.98 | 0.043 | 19.7 | 0.008 | 80.3 | 0.035 |
| M- <i>b</i> -S-5 | 97,100 | 2.46 | 5.3 | 0.609 | 68.5 | 0.417 | 31.5 | 0.192 |
| M- <i>b</i> -S-6 | 113,000 | 1.93 | 15.8 | 0.156 | 54.9 | 0.086 | 45.1 | 0.070 |
| M- <i>b</i> -S-7 | 152,400 | 4.41 | 36.7 | 0.038 | 70.6 | 0.027 | 29.4 | 0.011 |

 ${\it a} \ {\it Reaction condition: PMMA-L1-2: [MMA]_0/[SiO_2-Br]_0/[CuCl_2]_0/[dNbpy]_0/CuCl]_0 = 3000:1/4:0.4:8:3.6; PMMA-H1/M1/L3: [MMA]_0/[SiO_2-Br]_0/[CuCl_2]_0/[dNbpy]_0/[CuCl]_0 = 4000:1:0.4:8:3.6; M-b-S-1 \sim 2: [S]_0/[PMMA-H1/M1/L3: [MMA]_0/[SiO_2-Br]_0/[CuCl_2]_0/[MNA]_0/[MNA]_0/$

L1]₀/[CuBr₂]₀/[Me₆TREN]₀/[Sn(EH)₂]₀ = 50000:1/2:5:50:5; M-b-S-3~4: [S]/₀[PMMA-

 $L2]_0/[CuBr_2]_0/[Me_6TREN]_0/[Sn(EH)_2]_0 = 5000:1/2:0.5:5:0.5; M-b-S-5~7: [S]_0/[PMMA-D-S-5]_0/[PMMA-D-S-5]_0/[Sn(EH)_2]_0 = 5000:1/2:0.5:5:0.5; M-b-S-5~7: [S]_0/[PMMA-D-S-5]_0/[Sn(EH)_2]_0 = 5000:1/2:0.5:5:0.5$

 $H1/M1/L3]_0/[CuBr_2]_0/[Me_6TREN]_0/[Sn(EH)_2]_0 = 10000:1:2:20:2$ with 45 vol% anisole, 5 vol% DMF at 60 °C. b

Determined by SEC. $^cf_{\text{ino}}$ (inorganic content), determined by TGA. $^d\sigma$ (grafting density), calculated according to TGA data, e mol% fraction of PMMA blocks and PMMA-b-PS blocks in particle brushes, f Calculated according to TGA data, $\sigma = \sigma_1 + \sigma_2$, the deconvolution of SiO₂-g-PMMA-b-PS particle brushes polymer ligands SEC traces is shown in Table S3.

Transmission electron microscopy (TEM) was used to investigate the morphology of (approximately monolayer) particle brush films. Micrographs shown in Figure 1 illustrate the effect of extension efficiency for samples with about constant total grafting density of ~ 0.04 nm⁻². Figure 1a (M-*b*-S-1) corresponds to low extension efficiency of about 7 %. The resulting ultrasmall density of BCP tethers (0.003 nm⁻²) implies that a significant fraction of SiO₂-*g*-PMMA primary brush particles may remain unfunctionalized.⁵⁴ Correspondingly, Figure 1a reveals a phase-separated-type structure that was attributed to the separation of

PMMA and PMMA-PS modified brush particles. Spherical PS domains seen in the micrograph exhibited an average diameter of $\langle d \rangle \sim 185$ nm which is of the order of few multiples of the radius of gyration of the PS block. Increasing the fraction of BCP tethers, more uniform microstructures were observed. A common motif in Figures 1b-1d is the formation of string-like structures that bear similarity to anisotropic string structures that were observed previously for sparsely grafted homopolymer brush particles. ¹⁹ While string-like superstructures appear somewhat 'blurred' by irregular aggregation in the limit of low extension efficacies (M-b-

S-2, Fig. 1b), more discrete 'particle strings' are observed in the case of high extension efficacy (M-*b*-S-4, Fig. 1d). Contrast variation between intra- and inter-string regions in the micrographs suggest that particle cores are mostly concentrated within PMMA rich regions while PS-blocks segregate to the inter-string galley regions. We note that for all images a quantitative comparison between the areal fraction of components in TEM images and the respective composition based on TGA and DSC was performed to confirm the consistency of the interpretation (see Fig. S14-S20 and Table S1-S3).

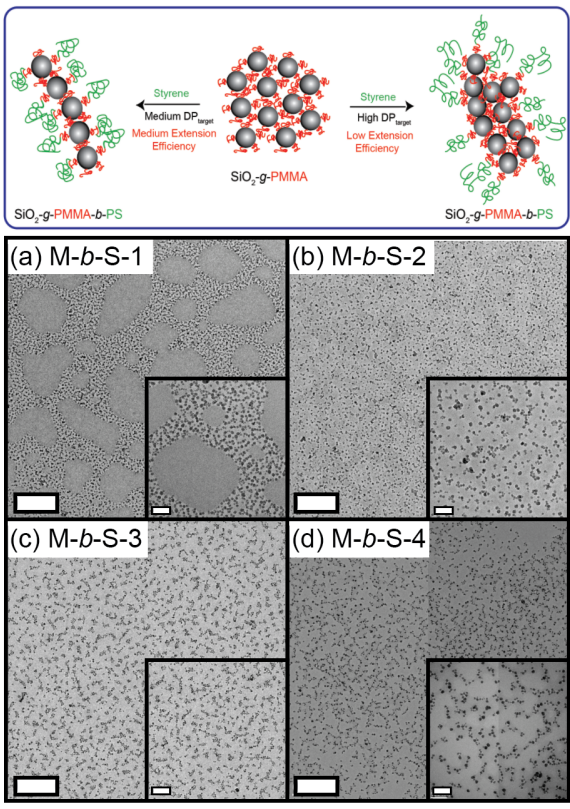


Figure 1. Schematic graph of the synthesis and assembly of bimodal SiO₂-g-PMMA/PMMA-*b*-PS particle brushes and TEM images of SiO₂-*g*-PMMA-*b*-PS particle brushes. (a) M-*b*-S-1, (b) M-*b*-S-2: (c) M-*b*-S-3: (d) M-*b*-S-4. Scale bar: 500 nm. inset scale bar: 100 nm.

The more irregular aggregate structures in the limit of low extension efficacy (M-*b*-S-1 and M-*b*-S-2, Fig. 1a and Fig. 1b) were interpreted as a consequence of a substantial amount of pristine primary SiO₂-*g*-PMMA particles. Since chain extension is expected to result in a binomial distribution of copolymer tethers among particles, the heterogeneity of modified particles increases rapidly in the limit of low extension efficacy.⁵⁴ For example, for primary SiO₂-*g*-PMMA particles with a grafting density of 0.04 chain/nm² and extension efficiency of 7% (M-*b*-S-1), about 20% of primary

particles are expected to not carry BCP tethers (calculated by equation S9). The phase separated structure for M-b-S-1 (Fig. 1a) and, similarly, the aggregate structures of M-b-S-2 and M-b-S-3 (Fig. 1b and 1c) suggest that pristine SiO₂-g-PMMA cluster within the PMMA rich regions of SiO₂-g-PMMA-b-PS. To validate this hypothesis, blending experiments of sparsely grafted SiO₂-g-PMMA particle brushes (PMMA-L2) with two SiO₂-g-PMMA-b-PS particle brushes (M-b-S-6 and M-b-S-4) were performed. As shown in Figure 2, after adding a large amount of SiO₂-g-PMMA particle brushes, the "string-like" structure of M-b-S-6 (Figure 2b) evolved to a "cluster-string" structure.

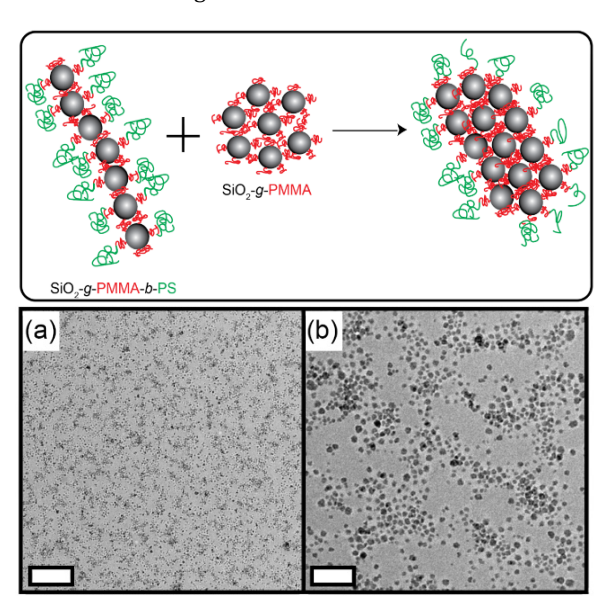
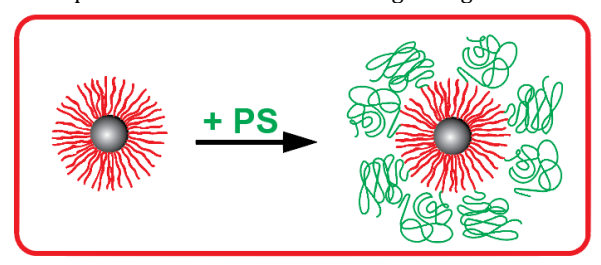
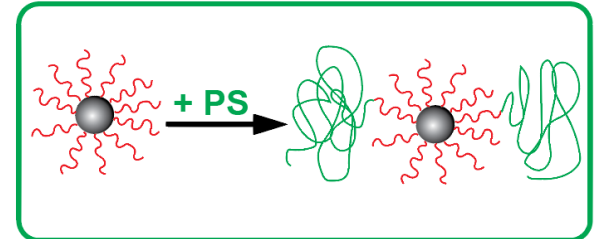


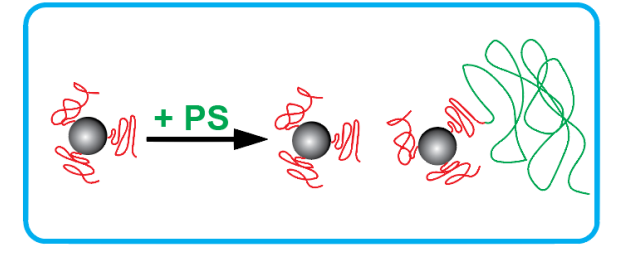
Figure 2. Schematic graph of the assembly of bimodal SiO₂-g-PMMA/PMMA-*b*-PS and SiO₂-*g*-PMMA particle brushes mixtures and TEM images of a mixture of SiO₂-*g*-PMMA-*b*-PS and SiO₂-*g*-PMMA particle brushes. (a-b) M-*b*-S-6 with PMMA-L2, mass ratio=1:4, scale bar: (a) 500 nm, (b) 100 nm.

Due to the lower grafting density of the added particle brushes, PMMA-L2, it is easy to distinguish the two distinct PMMA regions, one where the SiO₂-g-PMMA-b-PS particle brushes are located outside of the cluster and another where the SiO₂-g-PMMA particle brushes are inside the clusters. A similar evolution can be observed in sparsely grafted bimodal copolymer particle brush system (M-b-S-4) with a smaller PMMA phase (Figure S24). These observations not only support the proposed self-assembly mechanism but also demonstrate that adding SiO₂-g-PMMA particle brushes can enrich the PMMA phase in the system, overall enhancing the design and fabrication of unique and elaborate network structures.

. **Scheme 2**. Synthesis of bimodal SiO₂-g-PMMA/PMMA-*b*-PS particle brushes with different grafting densities.







Block copolymers can self-assemble into various morphologies after annealing.^{21, 55-57} The self-assembly of BCP-tethered brush particles is thus expected to be determined by the competition between excluded-volume type interactions (as they are present in regular homopolymer-brush particles) and the

microphase separation of copolymer tethers. Since the tethering of polymer chains to the particle surface restricts chain mobility and potentially limits the interaction between copolymer chains, the structure formation is expected to sensitively depend on brush characteristics such as grafting density. To evaluate the impact of graft composition and density, three SiO2-g-PMMA-b-PS particle brush systems were investigated to study the effect of chain composition and grafting density on the self-assembly of block copolymer particle brushes. First, three SiO₂-g-PMMA particle brushes (PMMA-H1/M1/L3) with different grafting densities (high: 0.75 nm⁻², medium: 0.15 nm⁻², low: 0.05 nm⁻²) but with a similar degree of polymerizations (DP~450 to 550) were prepared, Table 1. Before chain extension, the morphologies of SiO₂-g-PMMA particle brushes were characterized by TEM, Figure S14, which confirmed the expected decrease in particle distance with decreasing grafting density. The outer PS blocks were prepared by ARGET ATRP chain extension with the same initial macroinitiator concentration ([SiO₂-g-PMMA-Br]₀), (50 ppm referred to styrene monomers). Polymer ligands $(M-b-S-5\sim7)$ were characterized by SEC after etching the SiO₂ cores. The bimodal features and high dispersity values from the SEC traces (Figures S10-S12) indicated only a partial chain extension from the tethered PMMA blocks. After deconvolution of the SEC traces, the composition of polymer ligands (PMMA and PMMA-b-PS) are listed in Table S3, which shows that the fraction of PMMA-b-PS ligands prepared under these conditions was 30% to 45%, which also defines the re-initiation efficiency for the chain extension reaction of PS blocks. (Scheme 2)

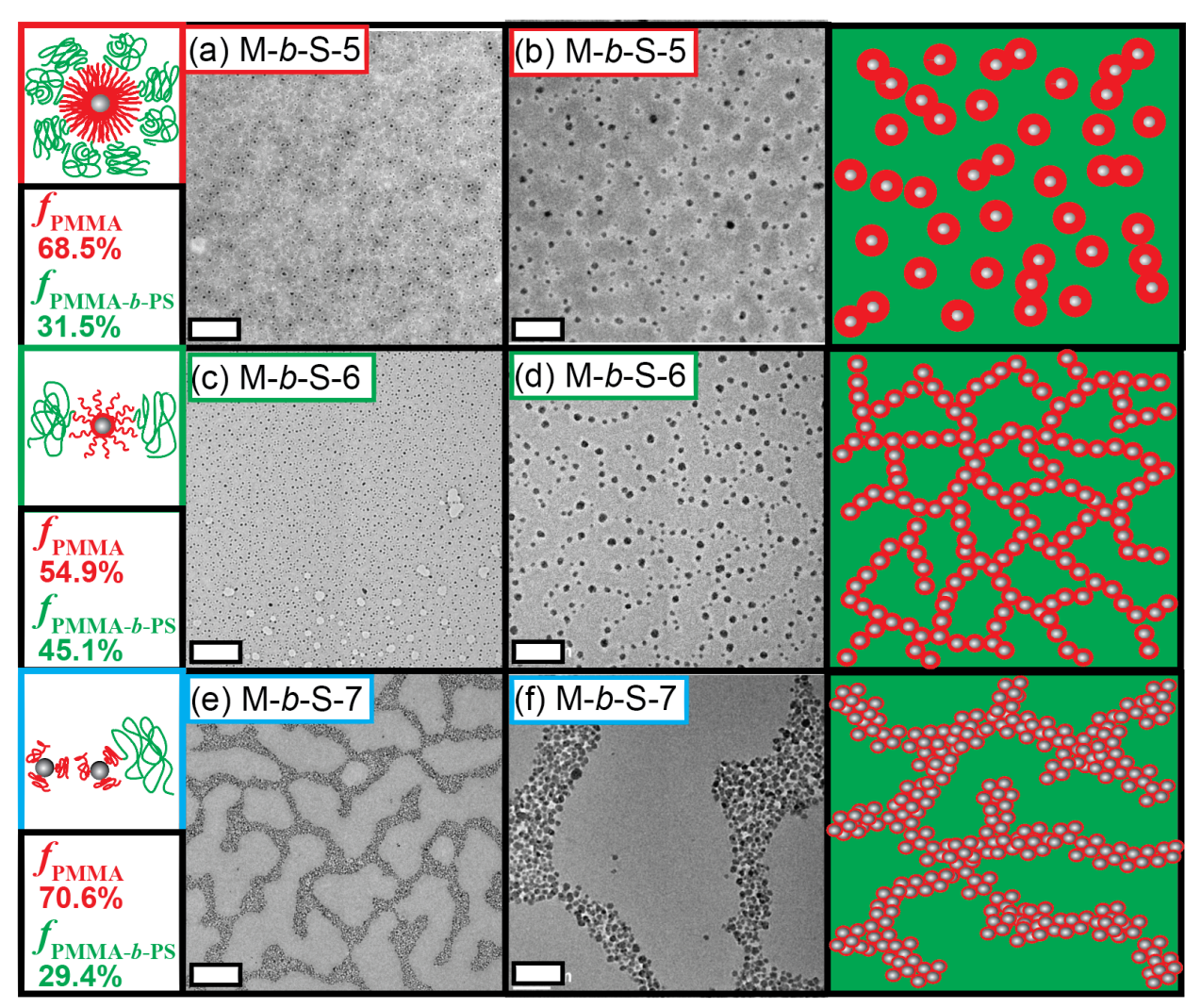


Figure 3. TEM images of SiO_2 -g-PMMA-b-PS particle brushes. (a-b) M-b-S-5, (c-d) M-b-S-6: (e-f) M-b-S-7. Scale bar, (a), (c), (e): 500 nm; (b), (d), (f), 100 nm.

Although the three BCP particle brushes (M-b-S-5, 6, 7) have comparable ligand compositions, i.e. similar PMMA blocks and block copolymer ligand fractions, their morphologies were dramatically different. To evaluate structure formation, thin films were solution cast onto carbon-coated Cu-grids and analyzed using electron imaging after thermal annealing for 24 h at T = 120 °C in vacuum and staining with RuO₄. Figure 3 shows the TEM images of M-b-S-5~7 particle brushes with the same magnification. The high grafting density particle brush (M-b-S-5) showed a relatively uniform structure with partially string-like features in the monolayer film on Cu grids, Figures 3a-b and Figure S22. In contrast, medium and low grafting density systems exhibited strongly anisotropic morphological features, such as connecting strings (M-b-S-6, Figures 3cd) and continuous cluster networks (M-b-S-7, Figures 3ef), respectively. This unique assembly behavior is attributed to the different grafting densities and resulting chain conformations of polymer ligands on the silica nanoparticle surfaces. The apparent grafting densities (σ_2) of PMMA-b-PS block, which are calculated using the grafting density of SiO₂-g-PMMA particle brush (σ_2 , Table 1) and the fraction of block copolymer ligands after chain extension are listed in Table S3. In the case of high grafting density particle brush systems, the grafting density of PMMA-b-PS ligands is 0.192 nm- 2 , which is still in the medium and high grafting density region. With sufficient PS outer layers, this leads to a relatively uniform structure.

Our results demonstrate that in the presence of a copper catalyst formed with highly activating ligands under a low ppm catalyst loading condition, SiO_2 -g-

PMMA/PMMA-b-PS particle brushes were successfully synthesized by SI-ATRP. The grafting density and concentration of the hybrid initiator, SiO₂-g-PMMA-Br, were effective parameters for the synthesis of bimodal chain composition via chain extension. Bimodal homo-/block copolymer particle brushes were thus obtained through simple chain extensions from PMMA grafted silica particle brushes. Within the tested regime of (rather small) grafting density, self-assembly of bimodal block copolymer tethered brush particles resulted predominantly in anisotropic string-like and continuous cluster network morphologies. The results suggested that structure formation was determined by the superposition of driving forces relating to the immiscibility of block domains and chain segregation similar to previously reported sparse homopolymer brush particles. For densely tethered PMMA brush particles sparsely extended with PS, the resulting morphology resembled those of sparse brush particles with an 'apparent core' comprised of the inorganic core and the inner PMMA shell. The self-assembly of BCPs grafted from strategically designed hybrid particles provides a new route toward hierarchically ordered quasi-one component materials in which structure results through the competition of hard-sphere type and block segregation-driven interactions. This provides new perspectives for the engineering of highperformance composite materials that require localized or specifically oriented particles, ultimately allowing for efficient capitalization of these materials' distinct properties.

ASSOCIATED CONTENT

Supporting Information. SEC traces of polymer PMMA/PS/PS-*b*-PMMA ligands. The Supporting Information is available free of charge on the ACS Publications website at (*tba*).

AUTHOR INFORMATION

Corresponding Author

- * E-mail: bockstaller@cmu.edu (M.R.B.).
- * E-mail: km3b@andrew.cmu.edu (K.M.).

Author Contributions

Z.W. synthesized materials and performed characterization work. Z.W., J.Y. S.L. T.L. and M.O. assisted in the synthesis; Y.Z and Y.L assisted in the characterization work. M.R.B. and K.M. conceived and organized the project and together with Z.W. wrote the manuscript. Z.W. and J.L. contributed equally.

Notes

The authors declare no competing financial interest. ACKNOWLEDGMENT

This work was supported by NSF (DMR 1501324 and DMR 1410845), the National Science Center (grant UMO-2014/14/A/ST5/00204), as well as the Scott Institute for Energy Technologies at Carnegie Mellon University. M.R. Bockstaller acknowledges support by the National Science Foundation *via* grants CMMI-1663305 (characterization of homopolymer-tethered brush particle films) and DMR-1709344 (characterization of block copolymer-tethered brush particle films). Zhenhua Wang gratefully acknowledges financial support from China Scholarship Council.

REFERENCES

- (1) Maillard, D.; Kumar, S. K.; Fragneaud, B.; Kysar, J. W.; Rungta, A.; Benicewicz, B. C.; Deng, H.; Brinson, L. C.; Douglas, J. F., Mechanical Properties of Thin Glassy Polymer Films Filled with Spherical Polymer-Grafted Nanoparticles. *Nano Lett.* **2012**, *12* (8), 3909-3914.
- (2) Kumar, S. K.; Benicewicz, B. C.; Vaia, R. A.; Winey, K. I., 50th Anniversary Perspective: Are Polymer Nanocomposites Practical for Applications? *Macromolecules* **2017**, *50* (3), 714-731.
- (3) Jancar, J.; Douglas, J. F.; Starr, F. W.; Kumar, S. K.; Cassagnau, P.; Lesser, A. J.; Sternstein, S. S.; Buehler, M. J., Current issues in research on structure–property relationships in polymer nanocomposites. *Polymer* **2010**, *51* (15), 3321-3343.
- (4) Zou, H.; Wu, S.; Shen, J., Polymer/Silica Nanocomposites: Preparation, Characterization, Properties, and Applications. *Chem. Rev.* **2008**, *108* (9), 3893-3957.
- (5) Mackay, M. E.; Tuteja, A.; Duxbury, P. M.; Hawker, C. J.; Van Horn, B.; Guan, Z.; Chen, G.; Krishnan, R. S., General Strategies for Nanoparticle Dispersion. *Science* **2006**, *311* (5768), 1740-1743.
- (6) Mahoney, C.; Hui, C. M.; Majumdar, S.; Wang, Z.; Malen, J. A.; N. Tchoul, M.; Matyjaszewski, K.; Bockstaller, M. R., Enhancing thermal transport in nanocomposites by polymer-graft modification of particle fillers. *Polymer* **2016**, *93*, 72-77.
- (7) Kumar, S. K.; Krishnamoorti, R., Nanocomposites: Structure, Phase Behavior, and Properties. *Annual Review of Chemical and Biomolecular Engineering* **2010**, *1* (1), 37-58.
- (8) Tchoul, M. N.; Dalton, M.; Tan, L.-S.; Dong, H.; Hui, C. M.; Matyjaszewski, K.; Vaia, R. A., Enhancing the fraction of grafted polystyrene on silica hybrid nanoparticles. *Polymer* **2012**, *53* (1), 79-86.
- (9) Vaia, R. A.; Maguire, J. F., Polymer Nanocomposites with Prescribed Morphology: Going beyond Nanoparticle-Filled Polymers. *Chem. Mater.* **2007**, *19* (11), 2736-2751.
- (10) Bockstaller, M. R.; Lapetnikov, Y.; Margel, S.; Thomas, E. L., Size-Selective Organization of Enthalpic Compatibilized Nanocrystals in Ternary Block Copolymer/Particle Mixtures. *J. Am. Chem. Soc.* **2003**, *125* (18), 5276-5277.
- (11) Lin, Y.; Böker, A.; He, J.; Sill, K.; Xiang, H.; Abetz, C.; Li, X.; Wang, J.; Emrick, T.; Long, S.; Wang, Q.; Balazs, A.; Russell, T. P., Self-directed self-assembly of nanoparticle/copolymer mixtures. *Nature* **2005**, *434* (7029), 55-59.
- (12) Bansal, A.; Yang, H.; Li, C.; Cho, K.; Benicewicz, B. C.; Kumar, S. K.; Schadler, L. S., Quantitative equivalence between polymer nanocomposites and thin polymer films. *Nat. Mater.* **2005**, *4* (9), 693-698.
- (13) Fernandes, N. J.; Koerner, H.; Giannelis, E. P.; Vaia, R. A., Hairy nanoparticle assemblies as one-component functional polymer nanocomposites: opportunities and challenges. *MRS Communications* **2013**, *3* (1), 13-29.

- (14) Yan, J.; Bockstaller, M. R.; Matyjaszewski, K., Brush-Modified Materials: Control of Molecular Architecture, Assembly Behavior, Properties and Applications. *Prog. Polym. Sci.* **2019**, 101180.
- (15) Jiao, Y.; Akcora, P., Assembly of Polymer-Grafted Magnetic Nanoparticles in Polymer Melts. *Macromolecules* **2012**, *45* (8), 3463-3470.
- (16) Jiao, Y.; Parra, J.; Akcora, P., Effect of Ionic Groups on Polymer-Grafted Magnetic Nanoparticle Assemblies. *Macromolecules* **2014**, *47* (6), 2030-2036.
- (17) Akcora, P.; Kumar, S. K.; García Sakai, V.; Li, Y.; Benicewicz, B. C.; Schadler, L. S., Segmental Dynamics in PMMA-Grafted Nanoparticle Composites. *Macromolecules* **2010**, *43* (19), 8275-8281.
- (18) LaNasa, J. A.; Torres, V. M.; Hickey, R. J., In situ polymerization and polymer grafting to stabilize polymer-functionalized nanoparticles in polymer matrices. *J. Appl. Phys.* **2020**, *127* (13), 134701.
- (19) Lee, J.; Wang, Z.; Zhang, J.; Yan, J.; Deng, T.; Zhao, Y.; Matyjaszewski, K.; Bockstaller, M. R., Molecular Parameters Governing the Elastic Properties of Brush Particle Films. *Macromolecules* **2020**.
- (20) Tang, S.; Horton, J. M.; Zhao, B.; Zhu, L., Self-organization of homopolymer brush- and mixed homopolymer brush-grafted silica nanoparticles in block copolymers and polymer blends. *Polymer* **2016**, *90*, 9-17.
- (21) Sarkar, B.; Alexandridis, P., Block copolymernanoparticle composites: Structure, functional properties, and processing. *Prog. Polym. Sci.* **2015**, *40*, 33-62.
- (22) Bockstaller, M. R.; Mickiewicz, R. A.; Thomas, E. L., Block Copolymer Nanocomposites: Perspectives for Tailored Functional Materials. *Adv. Mater.* **2005**, *17* (11), 1331-1349.
- (23) Liang, R.; Xu, J.; Li, W.; Liao, Y.; Wang, K.; You, J.; Zhu, J.; Jiang, W., Precise Localization of Inorganic Nanoparticles in Block Copolymer Micellar Aggregates: From Center to Interface. *Macromolecules* **2015**, *48* (1), 256-263.
- (24) Zhang; Horsch, M. A.; Lamm, M. H.; Glotzer, S. C., Tethered Nano Building Blocks: Toward a Conceptual Framework for Nanoparticle Self-Assembly. *Nano Lett.* **2003**, *3* (10), 1341-1346.
- (25) Cersonsky, R. K.; van Anders, G.; Dodd, P. M.; Glotzer, S. C., Relevance of packing to colloidal self-assembly. *Proc. Nat. Acad. Sci.* **2018**, *115* (7), 1439.
- (26) Lin, Y.; Daga, V. K.; Anderson, E. R.; Gido, S. P.; Watkins, J. J., Nanoparticle-Driven Assembly of Block Copolymers: A Simple Route to Ordered Hybrid Materials. *J. Am. Chem. Soc.* **2011**, *133* (17), 6513-6516.
- (27) Lee, J. Y.; Balazs, A. C.; Thompson, R. B.; Hill, R. M., Self-Assembly of Amphiphilic Nanoparticle–Coil "Tadpole" Macromolecules. *Macromolecules* **2004**, *37* (10), 3536-3539.
- (28) Phillips, C. L.; Glotzer, S. C., Effect of nanoparticle polydispersity on the self-assembly of polymer tethered nanospheres. *The Journal of Chemical Physics* **2012**, *137* (10), 104901.
- (29) Ma, S.; Qi, D.; Xiao, M.; Wang, R., Controlling the localization of nanoparticles in assemblies of amphiphilic diblock copolymers. *Soft Matter* **2014**, *10* (45), 9090-9097.
- (30) Li, Q.; Wang, Z.; Yin, Y.; Jiang, R.; Li, B., Self-Assembly of Giant Amphiphiles Based on Polymer-Tethered Nanoparticle in Selective Solvents. *Macromolecules* **2018**, *51* (8), 3050-3058.
- (31) Ma, S.; Hu, Y.; Wang, R., Amphiphilic Block Copolymer Aided Design of Hybrid Assemblies of Nanoparticles: Nanowire, Nanoring, and Nanocluster. *Macromolecules* **2016**, *49* (9), 3535-3541.

- (32) Marson, R. L.; Phillips, C. L.; Anderson, J. A.; Glotzer, S. C., Phase Behavior and Complex Crystal Structures of Self-Assembled Tethered Nanoparticle Telechelics. *Nano Lett.* **2014**, *14* (4), 2071-2078.
- (33) Wang, Y.; Cui, J.; Han, Y.; Jiang, W., Effect of Chain Architecture on Phase Behavior of Giant Surfactant Constructed from Nanoparticle Monotethered by Single Diblock Copolymer Chain. *Langmuir* **2019**, *35* (2), 468-477.
- (34) Santos, P. J.; Cheung, T. C.; Macfarlane, R. J., Assembling Ordered Crystals with Disperse Building Blocks. *Nano Lett.* **2019**, *19* (8), 5774-5780.
- (35) Zhang, T.; Fu, C.; Yang, Y.; Qiu, F., Phase Behaviors and Bridging Properties of Bolaform Tethered Nanoparticles. *Macromolecules* **2018**, *51* (5), 1654-1665.
- (36) Yue, K.; Huang, M.; Marson, R. L.; He, J.; Huang, J.; Zhou, Z.; Wang, J.; Liu, C.; Yan, X.; Wu, K.; Guo, Z.; Liu, H.; Zhang, W.; Ni, P.; Wesdemiotis, C.; Zhang, W.-B.; Glotzer, S. C.; Cheng, S. Z. D., Geometry induced sequence of nanoscale Frank–Kasper and quasicrystal mesophases in giant surfactants. *Proc. Nat. Acad. Sci.* **2016**, *113* (50), 14195-14200.
- (37) Guo, Y.; Harirchian-Saei, S.; Izumi, C. M. S.; Moffitt, M. G., Block Copolymer Mimetic Self-Assembly of Inorganic Nanoparticles. *ACS Nano* **2011**, *5* (4), 3309-3318.
- (38) Huang, Y.; Zheng, Y.; Sarkar, A.; Xu, Y.; Stefik, M.; Benicewicz, B. C., Matrix-Free Polymer Nanocomposite Thermoplastic Elastomers. *Macromolecules* **2017**, *50* (12), 4742-4753
- (39) Matyjaszewski, K.; Xia, J., Atom Transfer Radical Polymerization. *Chemical Reviews* **2001**, *101* (9), 2921-2990.
- (40) Matyjaszewski, K., Atom Transfer Radical Polymerization (ATRP): Current Status and Future Perspectives. *Macromolecules* **2012**, *45* (10), 4015-4039.
- (41) Zheng, Y.; Huang, Y.; Abbas, Z. M.; Benicewicz, B. C., One-pot synthesis of inorganic nanoparticle vesicles via surface-initiated polymerization-induced self-assembly. *Polym. Chem.* **2017**, *8* (2), 370-374.
- (42) Pyun, J.; Kowalewski, T.; Matyjaszewski, K., Synthesis of Polymer Brushes Using Atom Transfer Radical Polymerization.
 Macromolecular Rapid Communications 2003, 24 (18), 1043-1059.
 (43) Pietrasik, J.; Hui, C. M.; Chaladaj, W.; Dong, H.; Choi,
- J.; Jurczak, J.; Bockstaller, M. R.; Matyjaszewski, K., Silica-Polymethacrylate Hybrid Particles Synthesized Using High-Pressure Atom Transfer Radical Polymerization. *Macromolecular Rapid Communications* **2011**, *32* (3), 295-301.
- (44) Wang, Z.; Fantin, M.; Sobieski, J.; Wang, Z.; Yan, J.; Lee, J.; Liu, T.; Li, S.; Olszewski, M.; Bockstaller, M. R.; Matyjaszewski, K., Pushing the Limit: Synthesis of SiO2-g-PMMA/PS Particle Brushes via ATRP with Very Low Concentration of Functionalized SiO2-Br Nanoparticles. *Macromolecules* 2019, 52 (22), 8713-8723.
- (45) Li, Y.; Tao, P.; Viswanath, A.; Benicewicz, B. C.; Schadler, L. S., Bimodal Surface Ligand Engineering: The Key to Tunable Nanocomposites. *Langmuir* **2013**, 29 (4), 1211-1220.
- (46) Zhao, D.; Di Nicola, M.; Khani, M. M.; Jestin, J.; Benicewicz, B. C.; Kumar, S. K., Self-Assembly of Monodisperse versus Bidisperse Polymer-Grafted Nanoparticles. *ACS Macro Lett.* **2016**, *5* (7), 790-795.
- (47) Bozorgui, B.; Meng, D.; Kumar, S. K.; Chakravarty, C.; Cacciuto, A., Fluctuation-Driven Anisotropic Assembly in Nanoscale Systems. *Nano Lett.* **2013**, *13* (6), 2732-2737.
- (48) Kravchenko, V. S.; Potemkin, I. I., Self-assembly of rarely polymer-grafted nanoparticles in dilute solutions and on a surface: From non-spherical vesicles to graphene-like sheets. *Polymer* **2018**, *142*, 23-32.

- (49) Hui, C. M.; Pietrasik, J.; Schmitt, M.; Mahoney, C.; Choi, J.; Bockstaller, M. R.; Matyjaszewski, K., Surface-Initiated Polymerization as an Enabling Tool for Multifunctional (Nano)Engineered Hybrid Materials. *Chemistry of Materials* **2014**, *26* (1), 745-762.
- (50) Matyjaszewski, K.; Miller, P. J.; Shukla, N.; Immaraporn, B.; Gelman, A.; Luokala, B. B.; Siclovan, T. M.; Kickelbick, G.; Vallant, T.; Hoffmann, H.; Pakula, T., Polymers at Interfaces: Using Atom Transfer Radical Polymerization in the Controlled Growth of Homopolymers and Block Copolymers from Silicon Surfaces in the Absence of Untethered Sacrificial Initiator. *Macromolecules* 1999, 32 (26), 8716-8724.
- (51) Tsujii, Y.; Ohno, K.; Yamamoto, S.; Goto, A.; Fukuda, T., Structure and Properties of High-Density Polymer Brushes Prepared by Surface-Initiated Living Radical Polymerization. In *Surface-Initiated Polymerization I*, Jordan, R., Ed. Springer Berlin Heidelberg: Berlin, Heidelberg, **2006**, pp 1-45.
- (52) Ohno, K.; Morinaga, T.; Koh, K.; Tsujii, Y.; Fukuda, T., Synthesis of Monodisperse Silica Particles Coated with Well-Defined, High-Density Polymer Brushes by Surface-Initiated Atom

- Transfer Radical Polymerization. *Macromolecules* **2005**, *38* (6), 2137-2142.
- (53) Bombalski, L.; Dong, H.; Listak, J.; Matyjaszewsk, K.; Bockstaller, M. R., Null-Scattering Hybrid Particles Using Controlled Radical Polymerization. *Adv. Mater.* **2007**, *19* (24), 4486-4490.
- (54) Hakem, I. F.; Leech, A. M.; Johnson, J. D.; Donahue, S. J.; Walker, J. P.; Bockstaller, M. R., Understanding Ligand Distributions in Modified Particle and Particlelike Systems. *J. Am. Chem. Soc.* **2010**, *132* (46), 16593-16598.
- (55) Sundrani, D.; Darling, S. B.; Sibener, S. J., Guiding Polymers to Perfection: Macroscopic Alignment of Nanoscale Domains. *Nano Lett.* **2004**, *4* (2), 273-276.
- (56) Choi, J.; Gunkel, I.; Li, Y.; Sun, Z.; Liu, F.; Kim, H.; Carter, K. R.; Russell, T. P., Macroscopically ordered hexagonal arrays by directed self-assembly of block copolymers with minimal topographic patterns. *Nanoscale* **2017**, *9* (39), 14888-14896.
- (57) Berry, B. C.; Bosse, A. W.; Douglas, J. F.; Jones, R. L.; Karim, A., Orientational Order in Block Copolymer Films Zone Annealed below the Order–Disorder Transition Temperature. *Nano Lett.* **2007**, *7* (9), 2789-2794.

